Journal of Inorganic and General Chemistry
ZAAC
Zeitschrift für anorganische und allgemeine Chemie
www.zaac.wiley-vch.de
RESEARCH ARTICLE

DOI: 10.1002/zaac.202200119

# A Binuclear Cobalt Complex in the Electrochemical Water Oxidation Reaction

Sebastian Nestke,[a] Jessica Stubbe,[d] Robert Koehler,[c] Emanuel Ronge,[b] Uta Albold,[d] Wolfgang Vioel,[c] Christian Jooss,[b] Biprajit Sarkar,*[d, e] and Inke Siewert*[a]

*Dedicated to the celebration of 130 years of ZAAC*

The water splitting reaction represents an appealing approach to store solar energy. The $4e^-/4H^+$ oxidation of water generating $O_2$ is considered as the bottleneck in this reaction and usually requires a rather large over potential. We report on the synthesis and application of a binuclear cobalt(III) complex, **1**, with two μ-OH ligands and tripodal triazole ligands, L, in the electrochemical water oxidation reaction (WOR; L = tris((1-phenyl-1H-1,2,3-triazol-4-yl)methyl)amine). The cobalt(III) centres in the complex exhibit an octahedral coordination geometry and the complex is stable in water. Electrochemical studies revealed that solutions of $\mathbf{1}^{NO3}$ catalyse the WOR in phosphate or borate buffer. However, further analysis showed, that $\mathbf{1}^{NO3}$ is a precursor and decomposes under the applied potential. A smooth deposit is formed on the electrode surface, which is a highly active water oxidation catalysis. The deposit consists of mainly cobalt oxide/hydroxide, which accounts for the catalytic activity, and small amounts of $\mathbf{1}^{NO3}$.

## Introduction

Water splitting is an attractive way for solar energy storage in chemical bond energy. The oxygen evolution reaction in this process is associated with high barriers for some individual redox steps and kinetically slow due to the O–O bond formation step. Heterogeneous cobalt oxide has been investigated intensively as electrocatalysts in the electrochemical water oxidation reaction.[1] This prompted the synthesis of well-defined di- and multinuclear molecular analogues to obtain insight into the structure of key intermediates and the catalytic mechanism during water oxidation catalysis.[2] However, determining whether the homogeneous WOC remains intact under the harsh oxidative conditions of the electrolysis or is actually a precursor for heterogeneous WOC is a crucial question in these studies. $CoO_x$ is highly active and even hardly measurable amounts may serve as active species. For example, $[Co_2(TPA)_2(OH)(O_2)]^{3+}$ was reported by Wang et al. as homogeneous photo- and electrochemical water oxidation catalyst (Figure 1).[3] However, later studies indicated that the complex likely decomposes under certain conditions in the electro- or photochemical water oxidation catalysis and that $CoO_x$ is actually the main active species then.[4] By modifying the ligand set, that is changing from a $(py)_3,R_3N$ ligand set as in TPA to an $(py)_2,(R_3N)_2$ to increase the stability, no catalytic activity was observed.[4a] These studies prompted us to investigate binuclear cobalt complex with a triazole ligand, $\mathbf{1}^{NO3}$, in the electrochemical water oxidation reaction (Figure 1). Triazole ligands have become increasingly popular as they can be derived rather straight-forward via copper(I) catalysed click chemistry. They

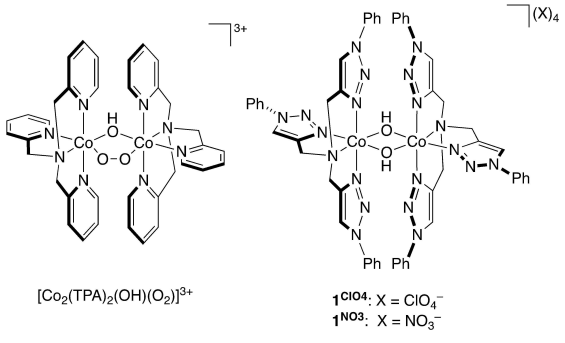


**Figure 1.** Binuclear cobalt complexes with μ-hydroxide ligands.

[a] S. Nestke, I. Siewert
Universität Göttingen, Institut für Anorganische Chemie, Tammannstr. 4, 37077 Göttingen, Germany
E-mail: inke.siewert@chemie.uni-goettingen.de
[b] E. Ronge, C. Jooss
Universität Göttingen, Institut für Materialphysik Chemie, Friedrich-Hund-Platz 1, 37077 Göttingen, Germany
[c] R. Koehler, W. Vioel
Hochschule für Angewandte Wissenschaft und Kunst Göttingen, Fakultät Ingenieurwissenschaften und Gesundheit, Von-Ossietzky-Straße 99, 37085 Göttingen, Germany
[d] J. Stubbe, U. Albold, B. Sarkar
Institut für Chemie und Biochemie, Freie Universität Berlin, Fabeckstraße 34–36, 14195, Berlin, Germany
[e] B. Sarkar
Lehrstuhl für Anorganische Koordinationschemie, Universität Stuttgart, Pfaffenwaldring 55, 70569, Stuttgart, Germany
E-mail: sarkar@iac.uni-stuttgart.de

can coordinate either as N or C donor ligand. Such complexes have been explored for a large variety of application including solar energy conversion reactions, light emitting compounds, or other catalytic applications.[5]

## Results and discussion

*Complex synthesis and characterisation.* The complex has been synthesised similar to the procedure that has been published previously for the related complex with benzyl instead of phenyl substituents in the ligand backbone.[6] $Co(ClO_4)_2$*$6H_2O$ and the ligand were dissolved in MeCN, subsequently, $H_2O_2$ was added, and the solution was stirred overnight. $\mathbf{1}^{ClO4}$, $[Co_2L_2(OH)_2](ClO)_4$), was isolated after work-up and purification as red solid in 24% yield. The NMR spectra reveals a diamagnetic compound and exhibits the expected signal set for a $C_{2h}$ symmetric complex. The $^1$H signal of the hydroxo-ligand appears as a singlet at 0.7 ppm. Formation of the dimer was supported by mass spectrometry and the complex has also been characterized by single X-ray diffraction. The results are depicted in Figure 2, Table 1, and details on X-ray refinement can be found in the SI. The cobalt(III) ions both exhibit a slightly distorted octahedral coordination geometry and are bridged by two hydroxide ligands (continuous shape measurement, CShM, for octahedral Co = 0.615[7]). The amine and one triazole unit coordinate in the equatorial position, the other two in the axial positions. The Co–O bond distances are within the range expected for a Co(III) low spin configuration and all bond lengths angles are similar to the one observed for the previous reported benzyl derivative of $\mathbf{1}^{ClO4}$.[6] Analysis by the bond valence method supported a low spin Co(III) configuration ($\Sigma$ = 3.06, see SI).[8]

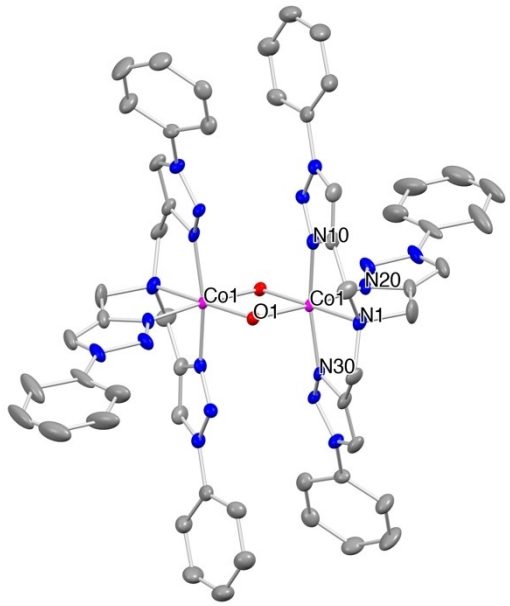


**Figure 2.** Molecular structure of $\mathbf{1}^{ClO4}$*4MeCN. $ClO_4^-$-ions, hydrogen atoms and solvent molecules were omitted for clarity. Thermal ellipsoids were set at the 50% level.

**Table 1.** Selected bond lengths /Å for $\mathbf{1}^{ClO4}$*4MeCN.

| Atoms | $\mathbf{1}^{ClO4}$ | Atoms | $\mathbf{1}^{ClO4}$ |
|---|---|---|---|
| Co1–O1 | 1.903(4) | Co1–N10 | 1.899(4) |
| Co1–O1′ | 1.918(4) | Co1–N20 | 1.890(5) |
| Co1–N1 | 2.011(4) | Co1–N30 | 1.922(3) |

*Water oxidation catalysis.* Since the water solubility of the perchlorate complex was limited, the nitrate complex $[Co_2L_2(OH)_2](NO_3)_4$, $\mathbf{1}^{NO3}$, was used for all further studies. All CV measurements in water have been referenced *vs.* NHE. The CV of $\mathbf{1}^{NO3}$ in aqueous phosphate buffer at pH = 7 with a glass carbon (GC) electrode exhibits a catalytic wave at $E_{p,1}$ = 1.53 V and a second slightly smaller wave at $E_{p,2}$ = 1.74 V (Figure S3, $\nu$ = 0.1 $Vs^{-1}$, $I$ = 0.1 M phosphate, $c_{1NO3} \approx 1$ mM). Upon successive CV scans the first wave vanishes and the second one shifts to slightly higher potentials, but the current holds rather constant (Figure S3). Polishing of the electrode re-establishes the initial CV (Figure S4). Changing to boron doped diamond (BDD) as electrode material did not have any impact, which indicates that the effect is not caused by changes of the carbon electrode surface under the harsh oxidative conditions, but an intrinsic property of the complex (Figure S5). Similar behaviour was observed at pH = 8: The CV data of $\mathbf{1}^{NO3}$ showed one catalytic wave at $E_{p,1}$ = 1.55 V, which also vanishes upon successive scanning and a second wave occurs at 1.8 V (Figure S6). The original CV was established after polishing the electrode (Figure S7). This indicates decomposition of the material during catalysis in phosphate-buffered water and formation of a heterogeneous material on the electrode surface, which is (also) active. This was corroborated by controlled potential electrolysis experiments (CPE). After CPE at 1.39 V for 15 minutes, the electrode was carefully taken out of the solution and a CV was recorded in a pure buffer solution (rinse test). The CV showed a large catalytic current, which is indeed characteristic for the deposition of an active material during CPE (Figure S8, Figure S9).

Since the buffer anion can have an impact on the stability and catalytic activity, catalysis with $\mathbf{1}^{NO3}$ was also investigated in boric acid. Indeed, the CV of $\mathbf{1}^{NO3}$ in aqueous boric acid at pH = 8 exhibits a catalytic wave at $E_{p1}$ = 1.43 V, which vanishes again upon successive scanning and a new one appeared at $E_{p,1}$ = 1.71 V (Figure S10), however, when the potential is switched at less oxidative potentials, the catalytic current holds constant and the peak shift is less pronounced (Figure 3). Over time the catalytic wave shifts to $E_{p1}$ = 1.35 V in the 10$^{th}$ cycle.

The CV data are not scan rate independent, which indicates that the catalysis is not under catalytic control and side phenomena occur (Figure S11). Concentration dependent measurements revealed a saturation behaviour of the maximum current at concentrations of above 0.25 mM and an S-shaped CV curve at 0.25 mM, which is indicative for catalysis under kinetic control (Figure S12).

CPE showed a large catalytic current, which decreased over time (Figure S13). Since the conductivity of the solution was rather low, 0.1 M sodium sulphate/0.1 M boric acid solution was

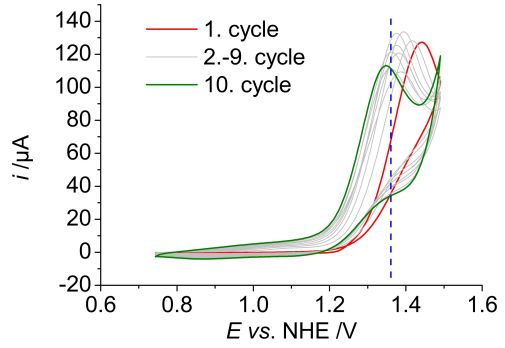


**Figure 3.** CV data of $\mathbf{1}^{NO3}$ in boric acid, pH = 8, GC electrode, $[\mathbf{1}^{NO3}] \approx 1$ mM, I = 0.1 M $BO_3^{3-}$, $\nu = 0.1$ $Vs^{-1}$.

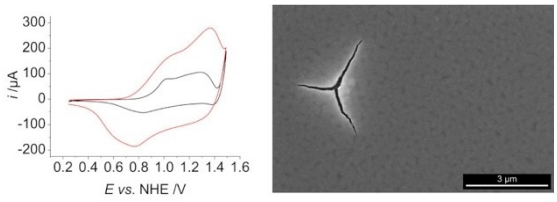


**Figure 4.** Left: CV of the re-used electrodes after CPE for 15 minutes, red $[\mathbf{1}^{NO3}] = 0.29$ mM, black $[Co(NO_3)_2] = 1.0$ mM, pH = 8, GC electrode, I = 0.1 M $B(OH)_3$ + 0.1 M $Na_2SO_4$, $\nu = 0.1$ $Vs^{-1}$. Right: SEM of the electrode surface after electrolysis.

used for further investigation. The current held constant then during CPE (Figure S14) and oxygen evolution was confirmed, however, the Faraday efficiency was rather low with 50% indicating that large amounts of the current end up in other processes. This prompted us to investigate the stability of $\mathbf{1}^{NO3}$ under catalytic conditions in more depth. The concentration of $\mathbf{1}^{NO3}$ decreased during electrolysis as confirmed by UV/Vis spectroscopy, which indicates that $\mathbf{1}^{NO3}$ partially decomposes during electrolysis also in boric acid (Figure S2). The rinse test indicated the formation of a catalytically active deposit. The CV of the electrode after CPE in a freshly prepared sodium sulphate/boric acid solution exhibit large catalytic currents (Figure S15). CPE with the re-used electrode in freshly prepared sodium sulphate/boric acid solution led to almost the same charge injection and FE indicating that the material deposited on the electrode surface is the sole active species (Figure S16).

In order to shed light on the active species, we also investigated a solution of cobalt(II) nitrate, which is known to be active in water oxidation catalysis, under similar conditions.[1a,2a] The CV of $Co(NO_3)_2$ in 0.1 M sodium sulphate/0.1 M boric acid solution showed a catalytic wave at $E_{p,1} = 1.36$ V ($\nu = 0.1$ $Vs^{-1}$, Figure S17), which is similar to the peak potential of the wave in the experiment with $\mathbf{1}^{NO3}$ in the 10$^{th}$ cycle. However, CPE at an applied potential of 1.36 V revealed a much lower current than for $\mathbf{1}^{NO3}$, although the concentration was three times higher (1.5 times higher normalized to the Co ion concentration, Figure S18). The CV of the electrode in boric acid solution after CPE exhibits the same features as after electrolysis of $\mathbf{1}^{NO3}$ indicating the formation of a similar material (Figure 4). Though, $\mathbf{1}^{NO3}$ seems to a better precursor than $Co(NO_3)_2$.

Scanning electron microscopy (SEM) of the electrode surface after CPE employing $\mathbf{1}^{NO3}$ showed that the electrode was all-over coated (Figure 4, Figure S19). The material was smooth with only a few cracks. EDX analysis indicated cobalt ions as main component (Figure S20). Since EDX is not sensitive for light elements, XPS was conducted in order to shed light on the composition of the material. For comparison, a dropcast sample of $\mathbf{1}^{NO3}$ was also investigated. Survey XPS showed that both samples consist of C, N, O, and Co atoms, as well as Si atoms, likely as an impurity from grease (Figure S21, Figure S22). In the dropcast sample, K and S atoms were also present. The detail XPS spectra of the N 1s peak are very similar in both samples, indicating that the deposit contains $\mathbf{1}^{NO3}$ (Figure S23, Figure S24). However, the molar ratio of N and Co atoms is much higher in the CPE sample, namely 1:0.80, than in the dropcats sample (cf. 1:0.14), which indicates that the deposit mainly consist of cobaltoxide/hydroxide and only minor amounts of $\mathbf{1}^{NO3}$. The binding energies of the 2p electrons of Co are only very little affected by the oxidation state of the metal centre, and thus it is not possible to distinguish between Co(II) and Co(III) ions, though, the satellite peaks at 785 eV indicate that Co ions in the oxidation state of +II are present.[9] Taking all measurements together, we conclude that the complex partially decomposes during electrolysis, forming cobalt(II) and/or cobalt(III) oxide and that this material is active in the WOC.

## Conclusion

The reaction of tris((1-phenyl-1H-1,2,3-triazol-4-yl)methyl)amine with Co(II) salts under oxidative conditions led to the formation of the dinuclear cobalt(III) complex with two bridging OH ligands. The complex was investigated in the water oxidation catalysis and solutions of $\mathbf{1}^{NO3}$ were very active, though with only moderate FE. Post catalytic analysis by XPS, SEM and EDX revealed that the complex decomposes during water oxidation catalysis and that a highly active cobalt oxide is formed on the electrode surface. The study highlights that careful post analysis is necessary to elucidate the active species in homogeneous, electrochemical water oxidation catalysis.

## Experimental Section

All Electrochemical measurements were recorded with a Gamry Instruments Reference 600 or Reference 600 Plus using degassed Millipore© water. A three-electrode setup was used with a glassy carbon (CH Instruments, $A = 7.1$ mm$^2$) or boron doped diamond (Windsor Scientific, $A = 7.1$ mm$^2$) working electrode, a platinum wire as counter electrode (99.999%, 1 mm diameter) and a SCE as reference electrode (ALS). All electrochemical data were referenced against NHE by adding 0.244 V. If not otherwise noted, before each scan the GC working electrode was pre-treated by rinsing with Millipore© water, 30 seconds polishing with an alox-slurry (0.05 µm), rinsing with Millipore© water, 3 minutes sonification in Millipore© water, rinsing with Millipore© water and drying. Electrolyte solution

(0.1 m) were prepared by titrating a 0.1 M $KH_2PO_4$ or 0.1 M $B(OH)_3$ with base. Unless otherwise noted, the electrolyte solution was stirred over Chelex® (100–200 mesh particle size, sodium form) for 20 minutes and the filtrate was used to improve the reproducibility. For the bulk electrolysis experiments, a glassy carbon rod (7 mm diameter) was used as working electrode and a platinum spiral as counter electrode. The electrolysis was conducted in a custom-made airtight two compartment cell. Working and counter electrode were separated by a porous glass frit. The working electrode was cycled 30 times between 1.84 V and −0.76 V with 500 $mVs^{-1}$ in electrolyte solution before electrolysis. The $O_2$ amounts in the CPE experiments were determined by a Shimadzu GC-2014 equipped with a TCD detector and a molecular sieves column. Methane was used as an internal standard in order to determine $n_{O2}$. The faradaic efficiency was determined by $n$-(measured)$_{O2}$/($Q$/4$F$), $Q$ = electric charge. A calibration curve for $CH_4/O_2$ was determined by injecting known quantities of the mixtures. GC plates (1 × 1 cm) were used for the electrolysis experiments with subsequent surface analysis.

$Co(ClO_4)_2 \cdot 6H_2O$ (183.0 mg, 0.5 mmol) and the ligand (0.5 mmol) were dissolved in MeCN (5 mL). The reaction mixture was stirred for 30 min and afterwards a 30% $H_2O_2$ solution (0.05 mL) was added. $\mathbf{1}^{\mathbf{ClO4}}$, $[Co_2L_2(OH)_2](ClO_4)_4$, precipitated during the reaction and could be obtained by filtration and washing with acetone. $\mathbf{1}^{\mathbf{NO3}}$, $([Co_2L_2(OH)_2](NO_3)_4$, was synthesized according to the same procedure using 0.5 mmol $Co(NO_3)_2 \cdot 6H_2O$ as precursor, and was obtained as orange-red solid. $^1$H NMR (401 MHz, $CD_3CN$, 22 °C): δ = 8.68 (s, 4H, ax. triazole CH), 8.01 (s, 2H, eq. triazole-CH), 7.53–7.62 (m, 10H, eq. phenyl), 7.25–7.41 (m, 20H, ax. phenyl), 5.40 (d, 4H, $J_{H-H}$ = 15.3, ax. $CH_2$), 4.82 (d, 4H, $J_{H-H}$ = 15.3, ax. $CH_2$), 4.43 (s, 4H, eq. $CH_2$), 0.74 (s, 2H, OH) ppm. $^{13}$C-NMR (101 MHz, $C_3D_7NO$, 21 °C): δ = 151.9, 150.2, 136.7, 136.1, 130.4, 130.2, 121.0, 118.6, 118.5 ppm; hr-ESI-MS: [$\mathbf{1}^{4+}$–$H^+$] 375.6740 (calc. 375.7665).

## Acknowledgements

I. S. thanks the DFG (SI 1577-2), Göttingen University, and the Fonds der Chemischen Industrie for financial support. We thank Robert Walter for the final refinement of the structure of $\mathbf{1}^{\mathbf{ClO4}}$. Open Access funding enabled and organized by Projekt DEAL.

## Conflict of Interest

The authors declare no conflict of interest.

## Data Availability Statement

The data that support the findings of this study are available in the supplementary material of this article.

**Keywords:** Cobalt · Coordination Chemistry · Electrocatalysis · N-Donor Ligands

[1] a) M. W. Kanan, D. G. Nocera, *Science* **2008**, *321*, 1072; b) Y. Surendranath, M. Dinca, D. G. Nocera, *J. Am. Chem. Soc.* **2009**, *131*, 2615; c) M. Risch, V. Khare, I. Zaharieva, L. Gerencser, P. Chernev, H. Dau, *J. Am. Chem. Soc.* **2009**, *131*, 6936; d) J. B. Gerken, J. G. McAlpin, J. Y. Chen, M. L. Rigsby, W. H. Casey, R. D. Britt, S. S. Stahl, *J. Am. Chem. Soc.* **2011**, *133*, 14431; e) J. Rosen, G. S. Hutchings, F. Jiao, *J. Am. Chem. Soc.* **2013**, *135*, 4516–4521; f) Deng, H. Tüysüz, *ACS Catal.* **2014**, *4*, 3701–3714; g) R. Wei, M. Fang, G. Dong, C. Lan, L. Shu, H. Zhang, X. Bu, J. C. Ho, *ACS Appl. Mater. Interfaces* **2018**, *10*, 7079–7086.

[2] For example: a) D. J. Wasylenko, C. Ganesamoorthy, J. Borau-Garcia, C. P. Berlinguette, *Chem. Commun.* **2011**, *47*, 4249–4251; b) D. K. Dogutan, R. McGuire, D. G. Nocera, *J. Am. Chem.* **2011**, *133*, 9178; c) D. M. L. Rigsby, S. Mandal, W. Nam, L. C. Spencer, A. Llobet, S. S. Stahl, *Chem. Sci.* **2012**, *3*, 3058–3062; d) Q. Yin, J. M. Tan, C. Besson, Y. V. Geletii, D. G. Musaev, A. E. Kuznetsov, Z. Luo, K. I. Hardcastle, C. L. Hill, *Science* **2010**, *328*, 342; e) J. J. Stracke, R. G. Finke, *ACS Catal.* **2013**, *3*, 1209–1219; f) I. Siewert, J. Galezowska, *Chem. Eur. J.* **2015**, *21*, 2780–2784; g) F. Song, R. More, M. Schilling, G. Smolentsev, N. Azzaroli, T. Fox, S. Luber, G. R. Patzke, *J. Am. Chem. Soc.* **2017**, *139*, 14198–14208; h) J. H. Xu, L. Y. Guo, H. F. Su, X. Gao, X. F. Wu, W. G. Wang, C. H. Tung, D. Sun, *Inorg. Chem.* **2017**, *56*, 1591–1598; i) H. Kotani, D. Hong, K. Satonaka, T. Ishizuka, T. Kojima, *Inorg. Chem.* **2019**, *58*, 3676–3682; j) A. Dey, V. Kumar, S. Pal, A. Guha, S. Bawari, T. N. Narayanan, V. Chandrasekhar, *Dalton Trans.* **2020**, *49*, 4878–4886; k) A. Dey, A. Guha, V. Kumar, S. Bawari, T. N. Narayanan, V. Chandrasekhar, *Dalton Trans.* **2021**, *50*, 14257–14263; l) D. d Boer, Q. Siberie, M. A. Siegler, T. H. Ferber, D. C. Moritz, J. P. Hofmann, D. G. H. Hetterscheid, *ACS Catal.* **2022**, *12*, 4597–4607.

[3] H. Y. Wang, E. Mijangos, S. Ott, A. Thapper, *Angew. Chem. Int. Ed.* **2014**, *53*, 14499–14502; *Angew. Chem.* **2014**, *126*, 14727–14730.

[4] a) J. W. Wang, P. Sahoo, T. B. Lu, *ACS Catal.* **2016**, *6*, 5062–5068; b) J. Lin, B. Ma, M. Chen, Y. Ding, *Chin. J. Catal.* **2018**, *39*, 463–471.

[5] a) J. G. Haasnoot, *Coord. Chem. Rev.* **2000**, *200–202*, 131–185; b) M. H. Klingele, S. Brooker, *Coord. Chem. Rev.* **2003**, *241*, 119–132; c) J. D. Crowley, D. A. McMorran, *"Click-Triazole" Coordination Chemistry: Exploiting 1,4-Disubstituted-1,2,3-Triazoles as Ligands.* In: Košmrlj J. (eds) Click Triazoles. Topics in Heterocyclic Chemistry, **2012**, *28.* Springer, Berlin, Heidelberg; d) P. I. P. Elliott, *Organomet. Chem.* **2014**, *39*, 1–25; e) D. Schweinfurth, L. Hettmanczyk, L. Suntrup, B. Sarkar, *Z. Anorg. Allg. Chem.* **2017**, *643*, 554–584; f) Q. V. C. van Hilst, N. R. Lagesse, D. Preston, J. D. Crowley, *Dalton Trans.* **2018**, *47*, 997–1002.

[6] D. Schweinfurth, J. Klein, S. Hohloch, S. Dechert, S. Demeshko, F. Meyer, B. Sarkar, *Dalton Trans.* **2013**, *42*, 6944–6952.

[7] A. Tuvi-Arad, G. Alon, D. Avnir, CoSyM, http://csm.ouproj.org.il, accessed 12.05.2022.

[8] Bond valence parameters: https://www.iucr.org/resources/data/data-sets/bond-valence-parameters, accessed 12.05.2022.

[9] S. L. T. Andersson, R. F. Howe, *J. Phys. Chem.* **1989**, *93*, 4913–4920.

Manuscript received: March 25, 2022
Revised manuscript received: May 12, 2022

 